Residual Oil Distribution in Sandstone with Different Permeability Scale During Water Flooding Process

Xin WANG[a], Qi ZHANG[ab], Jun YAO[b], Yongfei YANG[b], Zhonghai ZHOU[a], Liya Duan[a]
[a]Institute of Oceanographic Instrumentation, Shandong Academy of Sciences (SDIOI)
[b]School of Petroleum Engineering, China University of Petroleum (East China)

This paper was prepared for presentation at the International Symposium of the Society of Core Analysts held in Snowmass, Colorado, USA, 21-26 August 2016

ABSTRACT

Recently with the rapid development of digital core technology, applications are used in the practical oil and gas field production. To illustrate the effect of pore structure on micro-distribution of residual oil, sandstones with different kinds of pore structure were imaged under the resolution of 3.78μm during water flooding process using X-ray tomography. Based on cluster-size distribution of oil segmented from the tomography images and classification using shape factor and Euler number, transformation of oil distribution pattern in different injection stages has been studied for the samples with different pore structures, which demonstrated distinctly different evolution behaviors of oil cluster. In general, distribution patterns of oil cluster constantly change during imbibition. Large connected oil clusters break off into smaller segments. Residual oil saturation tends to increase as the pore structure becomes more complicated where large oil blobs are trapped in such systems. For cores with good pore connectivity, which showed the largest change of distribution pattern, the oil distribution is relatively simple, and clusters are always concentrated on one or two kinds of distribution patterns. Meanwhile, some disconnected clusters merge and lead to re-connection at the stage of a high water cut. While pore structure becomes compact and complex, residual nonwetting phase becomes static and is difficult to move, so that all distribution patterns coexist during whole displacement process. As EOR methods for reservoirs containing residual oil are greatly influenced by pore scale entrapment characteristics of the oil phase, this study improves our ability to further enhance oil recovery.

INTRODUCTION

With advancement in X-ray computed micro tomography (μCT) and increase in computational power, detailed information extracted from 3D CT images of rocks can be used to accurately study multiphase flow in porous media at representative conditions. Started with glass bead packs[1-4], reseachers obtained the images of cores after both drainage and imbibition in real rock systems.The experimental examinations focus on relative permeability[5], fluid distribution[6-11], capillary pressure measurements[12], oil recovery[13], or wettability [14-16]. When displacement is carried out by usual

waterflooding, the complex pore structure is responsible for trapping a large portion of the oil phase within the pores of the rock. This in turn impacts the overall flow behaviour, such as oil recovery. Therefore, understanding of transport properties in porous materials and their dependence on pore geometry is critical. In the earliest studies, clusters of all sizes were observed, with approximately power-law distributions[17]. Cluster size has been found that can range from a single pore to multiple-pore configurations[4, 10, 18]. More recently, a tendency for residual nonwetting-phase saturations to increase as porosity decreased was noted[9]. However, these experiments do not reveal the morphology change of trapped cluster.

To overcome this, We focus here on two-phase flow of high water cut period in sandstones at pore-scale in 3D with micro-computed tomography(μ-CT). Four sandstones samples of different permeability scale were selected to representative of different reservoir sandstones. We have imaged sequences of water flooding production steps to study on changes of residual oil distribution and improve fundamental understanding with which it will be possible to reduce S_{or} further.

METHODOLOGY

Experiments

To introduce the effect of pore structure on residual oil distribution in the investigation, relatively homogeneous sandstone samples of different permeabilities were used to model the different kinds of porous media. Permeability and porosity of the four water-wet systems are 48.53mD, 110.84mD, 430.03mD, 520.81mD, and 0.25, 0.23, 0.21, 0.20, respectively. As the rapid development of pore network model, this method can be used to determine pore body and throat size locations and distributions from high-resolution tomographic images. Characterizations of pore structure, such as pore radius, throat radius, and coordination number etc. are calculated based on pore network model.

Brine doped with 10wt% potassium iodide (to enhance CT contrast) is the brine, and crude oil mixed with 52.1wt% kerosene is used as oil phase. The viscosity of aqueous phase is 1.2 mPa·s and for oil phase it is 0.75 mPa·s. Initially, the dry samples were scanned in order to obtain an accurate mapping of pore structure. Then the cores saturated with brine were displaced by oil until water production ceased. After ageing, the cores were scanned again to obtain the distribution of oil phase at connate oil saturation (So) state. Thirdly, the core plug was waterflooded by brine with a velocity of 0.1ml/min, and μCT images with a resolution of 3.78μm at 1PV, 5PV, 15PV, 50PV injection stages were then acquired respectively. All experiments were conducted at 297.15K and 0.1MPA.

The raw CT images were filtered and segmented by image filters and segmentation algorithms available within the commercial software package Avizo. Note that for each process step the same areas of $300\times300\times300 pixel^3$ are compared.

Characterization of residual oil

Residual oil distribution we got from the experimental CT images can be separated into a new image of the oil phase only, where disconnected blobs are labeled by distinct numerical values starting from the value of one to the maximum number of individual

blobs in the image. Then, attributes of every individual oil blob such as volume and interfacial area can be computed by performing operations on these sets of voxels.
There are two important parameters that we use to classify the distribution pattern. One is the sphericity index(G) which describes how closely an oil blob resembles a sphere. For a perfect sphere, G=1. It is computed as follows[19]:

$$G = \frac{6\sqrt{\pi}V}{S^{1.5}}$$

Where S is the surface area of the oil cluster and V is the volume of the oil cluster.
Another is the Euler number(E) which can be used as a characteristic describing the topological properties of the residual oil clusters. Euler number can be expressed by three Betti number[20].

$$E = b_0 - b_1 + b_2$$

Where E is the Euler number of oil cluster, b_0 is the number of isolated components, b_1 is the number of tunnels, b_2 is the number of cavities.
Combine the sphericity index (G) and Euler number(E) so that distribution pattern of residual oil can be defined(Table 1), as shown in Fig. 1.

Distribution pattern	
Network	G<0.1
Branch	0.1<G<0.3
Multiple	0.3<G<0.7 & E_N<1
Singlet	G>0.7
Film and tubular	0.3<G<0.7 & E_N≥1

Table 1 Classification of distribution patterns of micro residual oil

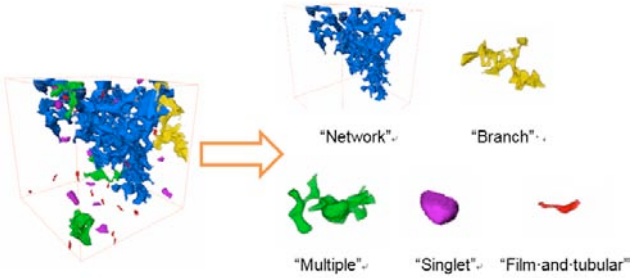

Fig. 1 Distribution patterns of oil cluster

RESULTS AND DISCCUSION

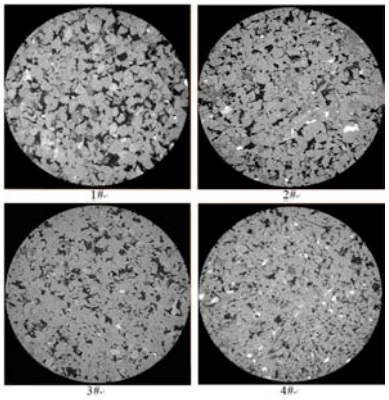

Fig. 2 Cross sections of the 4 sandstone samples

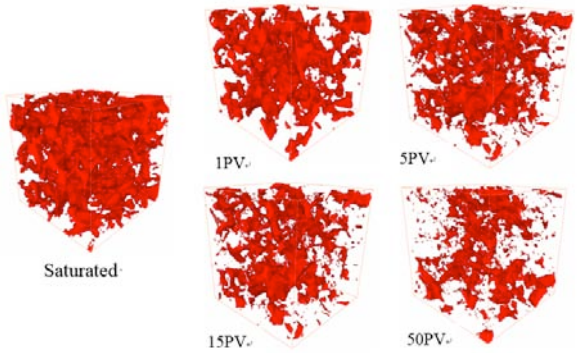

Fig. 3 Three-dimensional visualization of residual oil (sample 1#)

Fig. 2 shows the cross sections of the samples. As the permeability and porosity of the samples reduce, the pore structure getting complex, the pore connectivity poor, middle pores, small pores and fine throats develop and are short of big pores. Then portion of the original CT images of 300×300×300 voxels were extracted to segment and built into pore network. Table 2 shows parameters obtained by pore network characterization. As the

permeability and porosity of the samples reduces, the pore structure changes. Mean volume of pore and throat decreases, mean tortuosity has a tendency to increase, and mean coordination shows a decrease tendency. Mean pore radius and throat radius get smaller, and throat radius changes more than pore radius.

Table 2 Parameters of the samples abtained by pore network characterization

	1#	2#	3#	4#
Number of pores	598	4102	3175	3981
Mean pore radius(um)	25.37	11.30	10.99	8.15
Number of throats	1061	7649	5832	6718
Mean throat radius(um)	17.06	8.43	7.99	6.63
Mean coordination number	3.47	3.70	3.64	3.34
Mean Tortuosity	2.26	2.20	2.31	2.35
porosity(%)	22.29	20.33	18.47	13.67

As the complication pore structure, the decreased tendency of residual oil saturation become slower during water flooding process. Three-dimensional visualization of residual oil(Fig. 3) shows that the volume of residual oil reduces and its distribution patterns constantly change. The volume fraction of each pattern at each stage is calculated

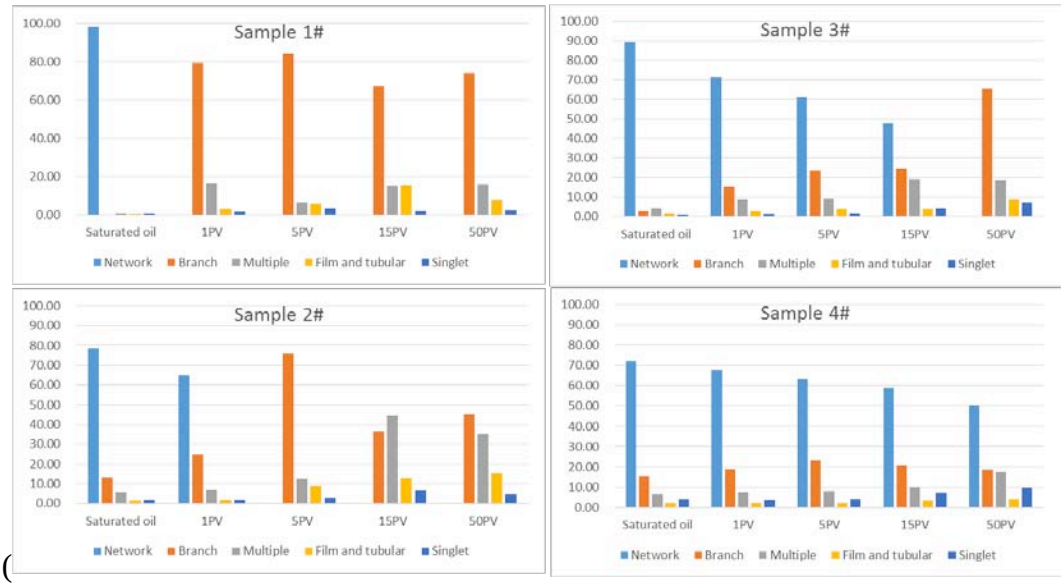

(Fig. 4).

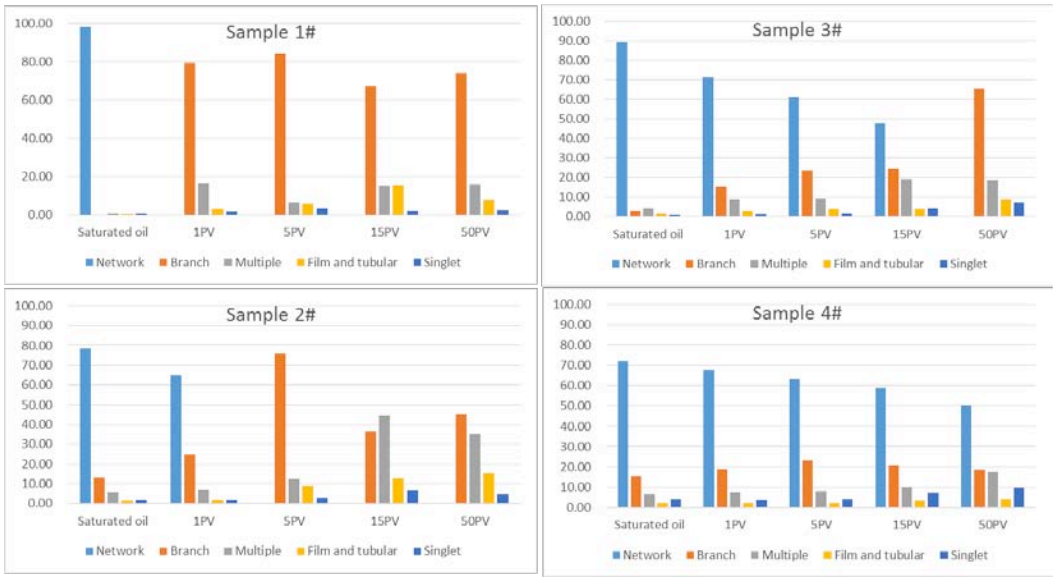

Fig. 4 Change of distribution pattern during water displacement

Sample 1# which has good connectivity between pores and throats has biggest changes in terms of the distribution pattern of residual oil. There is one dominating oil cluster in "network" form, which initially contains 99% of the total oil volume and is connected across the whole sample, disappeared after displacement. This could be because of the oil cluster breakup affected by snap-off events. Distribution pattern mainly is "branched" form after injection of 50PV brine.

Sample 2#, similar to sample 1#, due to affection of pore structure, prime distribution patterns are "branched" form and "multiple" form after injection of 50PV brine. We also observed a transition from a connected oil phase flow to disconnected clusters. In this process, the oil volume of "branched" rises sharply when "network" form of oil disappeared. Furthermore, redistribution of residual oil can be observed after 15 pore volume of water flooding displacement. Volume of "branch" form increases when the volume of "multiple" form decreases, this may be because of the coalescence events.

By contrast, water flooding displacement do not work well on sample3# and sample 4#which have more complicated pore structure. Their residual oil distribution patterns change less while oil clusters distribution is more complex. Especially 4# sample. All five distribution patterns coexist during whole displacement process, and mainly is "network" form.

CONCLUSION

Digital core technology is used to investigate the characteristics of residual oil clusters. The finding indicate that distribution of residual oil is influenced by pore structure and injected fluid volumes. Low permeability sandstones cores were more likely to have smaller pore radius, smaller throat radius, and poor coordination number which making process of oil production encounter greater resistance.

In imbibition, volume of residual oil in the pore space reduce, distribution patterns of oil clusters constantly change during displacement process. Cores with good pore

connectivity have biggest changes in terms of the distribution pattern of residual oil. Transition from a connected oil phase to disconnected clusters can be observed during water flooding. Oil volume of “branched”, “multiple” rise sharply when “network” form of oil disappeared at the stage of a high water cut. Residual oil distribution pattern of cores with compact pore structure has smaller change while oil clusters distribute more complex. All five distribution patterns coexist during whole displacement process, and mainly is “network” form. As EOR methods for reservoirs containing residual oil are greatly influenced by pore scale entrapment characteristics of the oil phase, this study should result in improvements in our ability to further enhance oil recovery.

ACKNOWLEDGEMENTS

We would like to express appreciation for the following financial support: International Science & Technology Cooperation Program of China (2014DFR60490), Chinese National Natural Science Foundation (51504146), Youth Scholar Foundation of Shandng Academy of Scienses (2014QN030) & (2015QN016).

REFERENCES

1. Culligan, K., et al., *Pore-scale characteristics of multiphase flow in porous media: a comparison of air–water and oil–water experiments.* Advances in water resources, 2006. **29**(2): p. 227-238.
2. Culligan, K.A., et al., *Interfacial area measurements for unsaturated flow through a porous medium.* Water Resources Research, 2004. **40**(12).
3. Geistlinger, H., et al., *Quantification of capillary trapping of gas clusters using X‐ray microtomography.* Water Resources Research, 2014. **50**(5): p. 4514-4529.
4. Karpyn, Z.T., M. Piri, and G. Singh, *Experimental investigation of trapped oil clusters in a water‐wet bead pack using X‐ray microtomography.* Water Resources Research, 2010. **46**(4).
5. Ghosh, J. and G.R. Tick, *A pore scale investigation of crude oil distribution and removal from homogeneous porous media during surfactant-induced remediation.* Journal of contaminant hydrology, 2013. **155**: p. 20-30.
6. Rücker, M., et al., *From connected pathway flow to ganglion dynamics.* Geophysical Research Letters, 2015.
7. Krummel, A.T., et al., *Visualizing multiphase flow and trapped fluid configurations in a model three‐dimensional porous medium.* AIChE Journal, 2013. **59**(3): p. 1022-1029.
8. Berg, S., et al. *Multiphase Flow in Porous Rock imaged under dynamic flow conditions with fast X-ray computed micro-tomography*. in *EGU General Assembly Conference Abstracts*. 2013.
9. Al-Raoush, R.I., *Experimental investigation of the influence of grain geometry on residual NAPL using synchrotron microtomography.* Journal of Contaminant Hydrology, 2014. **159**(0): p. 1-10.
10. Kumar, M., et al., *Visualizing and quantifying the residual phase distribution in core material.* Petrophysics, 2010. **51**(05).

11. Georgiadis, A., et al., *Pore-scale micro-computed-tomography imaging: Nonwetting-phase cluster-size distribution during drainage and imbibition.* Physical Review E, 2013. **88**(3): p. 033002.
12. Youssef, S., et al., *Investigation of Pore Structure Impact on the Mobilization of Trapped Oil by Surfactant Injection.*
13. Iglauer, S., et al. *In-situ Residual Oil Saturation And Cluster Size Distribution In Sandstones After Surfactant Flooding Imaged With X-ray Micro-computed Tomography*. in *International Petroleum Technology Conference*. 2014. International Petroleum Technology Conference.
14. Andrew, M., B. Bijeljic, and M.J. Blunt, *Pore-scale contact angle measurements at reservoir conditions using X-ray microtomography.* Advances in Water Resources, 2014. **68**: p. 24-31.
15. Al-Raoush, R.I., *Impact of wettability on pore-scale characteristics of residual nonaqueous phase liquids.* Environmental science & technology, 2009. **43**(13): p. 4796-4801.
16. Kumar, M., et al. *Quantifying trapped residual oil in reservoir core material at the pore scale: Exploring the role of displacement rate, saturation history and wettability*. in *International Petroleum Technology Conference*. 2009.
17. Iglauer, S., et al., *Comparison of residual oil cluster size distribution, morphology and saturation in oil-wet and water-wet sandstone.* Journal of Colloid and Interface Science, 2012. **375**(1): p. 187-192.
18. Iglauer, S., A. Paluszny, and M.J. Blunt, *Simultaneous oil recovery and residual gas storage: A pore-level analysis using in situ X-ray micro-tomography.* Fuel, 2013. **103**(0): p. 905-914.
19. Li, F., et al., *CT Experiments and Image Processing for the Water-Oil Displacement at Pore Scale.* Procedia Engineering, 2012. **29**: p. 3831-3835.
20. Kong, T.Y. and A. Rosenfeld, *Digital topology: Introduction and survey.* Computer Vision, Graphics, and Image Processing, 1989. **48**(3): p. 357-393.